Materials Advances

ROYAL SOCIETY OF CHEMISTRY

COMMUNICATION

View Article Online
View Journal | View Issue

Check for updates

Cite this: *Mater. Adv.*, 2022, 3, 7501

Received 31st May 2022,
Accepted 22nd August 2022

DOI: 10.1039/d2ma00614f

rsc.li/materials-advances

Treatment of nonwoven polypropylene to increase adsorption of SARS-CoV-2 spike protein†

Justin Gangwish, [a] Abhishek Bhattacharjee,[a] Roberta M. Sabino, [a] Vignesh K. Manivasagam,[b] Yan Vivian Li, [acd] Ketul C. Popat, [abd] Melissa Reynolds [def] and Susan James*[abd]

The COVID-19 pandemic caused by the respiratory transmission of the SARS-CoV-2 virus has resulted in millions of deaths. While the production of a vaccine has greatly reduced mortality and hospitalization where available, lack of vaccine availability and mutations of the virus render masking a vital strategy for reducing the spread of disease. Increasing the efficacy of a mask to adsorb the virus has significant potential to reduce disease spread. Nonwoven polypropylene (PP) is used as a filtration layer in N-95 masks and other over the counter masks. To increase the adsorption of the virus, the nonwoven PP layer was treated with oxygen plasma, polyethylene glycol (PEG), and hyaluronic acid (HA). The treated materials were evaluated over one month and found to increase adsorption of the spike protein on the surface of the SARS-CoV-2 virion.

Introduction

As of July 2022, the Centers for Disease Control and Prevention (CDC) have reported over a million deaths attributed to COVID-19 in the US.[1] The CDC recommends healthcare personnel who work with COVID-19 patients wear personal protective equipment (PPE) including gloves, isolation gowns, N95 respirators, and goggles/face shield to protect themselves from infection.[2] While PPE prevents healthcare personnel from being infected, it can also encourage the spread of disease between patients through contact transmission.[3,4] Polypropylene (PP), polyethylene (PE), and polyethylene terephthalate (PET) are materials commonly used to make isolation gowns and N95 masks.[5–8] These plastics are easily manufactured into PPE, but recent evidence has shown that plastic, PP in particular, provides SARS-CoV-2 viability up to 72 hours.[9] While new materials for PPE could be investigated to decrease the viability of SARS-CoV-2, it will take years to fully investigate, design, and manufacture novel materials. Alterations to current PPE materials, specifically nonwoven polypropylene used as a filtration layer in masks would be much faster, and our research group has already developed a method for incorporating a non-toxic and potentially viricidal biological polymer, hyaluronic acid, into plastics.[10–13] Furthermore, we have developed two cost effective methods to increase spike protein adhesion to nonwoven PP. The methods used to alter the nonwoven PP are well studied and documented to be non-toxic. Oxygen plasma treatment of polypropylene is a well-documented method for use in blood filtration and wound dressing.[14–17] PEG is widely used in drug delivery and has been evaluated for cytotoxicity.[18–21] Finally hyaluronic acid is a naturally occurring polymer that our group has extensively evaluated for cytotoxicity and have been successfully implanted in multiple large animal models.[10,13,22,23]

Experimental section

Plasma grafting peg onto nonwoven PP treatment

The nonwoven PP filtration layer of the fabric used in disposable face masks (Makena) was activated with oxygen plasma (PlasmaEtch) for 60 seconds. Immediately after activation, PP samples were placed in a 25 g L^{-1} solution of PEG (MW 3,350 kDa, Sigma Aldrich) in 200 proof ethanol for 15 minutes allowing the PEG to adsorb to the activated surfaces. Samples were dried under vacuum (−635 mmHg, all reported pressures are gauge pressure) for 10 minutes. The adsorbed PEG was grafted to the surface with a second oxygen plasma treatment for 300 seconds. Excess PEG was removed by 15 minutes of rinsing in methanol followed by a rinsing in ethanol for 15 minutes. Finally, the PP samples were dried under vacuum

[a] *School of Advanced Materials Discovery, Colorado State University, Fort Collins, USA. E-mail: Susan.James@colostate.edu*
[b] *Department of Mechanical Engineering, Colorado State University, Fort Collins, USA*
[c] *Department of Design and Merchandising, Colorado State University, Fort Collins, USA*
[d] *School of Biomedical Engineering, Colorado State University, Fort Collins, USA*
[e] *Department of Chemistry, Colorado State University, Fort Collins, USA*
[f] *Department of Chemical and Biological Engineering, Colorado State University, Fort Collins, USA*

† Electronic supplementary information (ESI) available. See DOI: https://doi.org/10.1039/d2ma00614f

(−635 mmHg) for 10 minutes. Sham PEG controls underwent the same process except the shams were submerged only in ethanol rather than a PEG/ethanol solution after the plasma activation step.

Hyaluronic acid complexed with cetyltrimethylammonium (HA-CTA) spray treatment

Sodium hyaluronate (Lifecore Biomedical) and cetyltrimethylammonium bromide (CTAB, Sigma Aldrich) were dissolved in DI at 0.3% (*w*/*v*) and 1.0% (*w*/*v*) respectively. The solutions were mixed, and the precipitate (HA-CTA) was collected, washed with DI water (5 times), dried under vacuum (−635 mmHg, 12 hours), and cryoground at −196 °C into a powder. The HA-CTA powder was dissolved in 200 proof ethanol at 0.4% (*w*/*v*) and 50 °C for 3 hours. The HA-CTA/ethanol solution was sprayed onto the nonwoven PP layer at 25–30 PSI using an airbrush (Powermate). The solution sprayed at 0.1 ml cm^{-2} which correlates to a deposition of HA-CTA at 0.4 mg cm^{-2}. The material was flipped, and the process repeated for the second side of the PP material. The sample was dried for 1 hour under vacuum at 635 mmHg.

A 2% (*v*/*v*) solution of toluene diisocyanate (TDI, Sigma Aldrich) in xylenes was prepared. The dry HA-CTA sprayed PP material was cut into circles approximately 6.35 cm in diameter and allowed to crosslink in the vapor above 10 ml of the TDI/xylene solution at 60 °C for 1 hour. The crosslinked samples were dried under vacuum overnight at −635 mmHg. After drying, the samples were hydrolyzed by placing each sample in 20 ml of 0.2 M NaCl in DI/ethanol (1 : 1, v/v) solution and sonicating for 1 hour. The solution was changed and the sonication repeated 3×. Samples were placed in 20 ml of DI/ethanol (3 : 2, v/v) for 2 hours, followed by sonication in DI for 30 minutes. Finally, samples were dried under vacuum (−635 mmHg) overnight.

Control samples

Control samples were untreated but opened and stored in ambient conditions to reflect storage conditions for the treated samples.

Attenuated total reflectance-Fourier transform infrared spectroscopy (ATR-FTIR)

ATR-FTIR (Nicolet 6700) spectra were taken on days 1, 7, 14, 21, and 28 after treatment. Samples were placed on the ATR crystal and run for 32 scans on the spectrometer. ATR-FTIR is known to penetrate a sample 0.5–2 microns depending on the material being tested,[24] due to this depth of penetration the FTIR curves shown present material properties in the bulk more so than atomic surface properties. Samples were stored in ambient conditions after treatment.

Contact angle goniometry

PP fabric contact angles were assessed by depositing a droplet of water on the surface taking the static contact angle over 5 minutes to determine if the material absorbed the water and the rate at which the contact angle changed as the material structure interacted with the droplet of water. Contact Angle was taken on days 1, 7, 14, 21, and 28 after treatment.

X-Ray photoelectron spectroscopy (XPS)

A PHI-5800 spectrometer with a monochromatic Al-K X-ray source operated at 15 kV was used to analyze the surface chemistry. Survey spectra were collected from 0 to 1100 eV with a pass energy of 187.85 eV. High-resolution spectra were collected for oxygen (O 1s) and Carbon (C 1s) from 280 to 294 eV and 526 to 538 eV, respectively. The atomic composition of the PP samples was calculated using peak fit analysis with Multipack software. Before taking spectra, samples were dried under vacuum (−635 mmHg) overnight. Spectra were collected every 7 days from day 1 to day 28.

Tensile property evaluation

Tensile testing was performed according to ASTM D3822.[25] Dog bone samples were punched from the material with a gauge length of 15 mm and a width of 3.16 mm. The samples were pulled at a constant rate of extension of 10%/min (1.5mm min^{-1}) until failure. The Youngs' modulus was calculated from 1–3% strain where all samples exhibited linear behavior. Testing was performed on an Instron 4442 with a 50 N load cell.

Water vapor transmission rate (WVTR)

W3/062 Water Vapor Transmission Rate Test System (Labthink, Boston, USA) was used which provided the WVTR in units of g m^{-2}-day. ASTM D6701-16 method was followed to conduct the experiment.[26] WVTR was collected on days 1, 14 and 28. Relative humidity of the instrument was between 55–60%. After each test, the samples were kept inside a ziplock bag at room temperature.

Spike protein adsorption

Samples were stored in ambient conditions for 14 days to simulate a brief period of storage before testing. Prior to ELISA studies, all samples were sterilized using sterile PBS and incubated in protein solution (1 μg ml^{-1}) for 2 h using a low attachment well plate. Protein solution was also incubated in empty wells as a positive control (the least adsorption possible). After this, the supernatants were collected and diluted 200-fold with assay buffer to obtain a protein solution in the standard curve range. The standard curve was obtained previously using the standards provided by the manufacturer (Sinobiological). The solutions' concentrations were then measured following the ELISA protocol. A more detailed section can be found in ESI.†

Cytotoxicity assay

Samples were assessed for cytotoxicity using an LDH (Lactate Dehydrogenase) assay. Samples were rinsed using PBS (Phosphate-buffered saline) and sterilized using UV light for 15 mins. Smooth muscle cells were grown for 24 hours on the surface of each sample. After 24 hours of incubation with the cells, 50 μL LDH reagent was added to 50 μL of incubated cell solution and allowed to react for 30 minutes. Later 50 μL stop

solution was added to each well and the absorbance was measured at 600 nm using a plate reader (BMG Labtech FLUOstarOmega). A negative control was used to determine the maximum LDH release, in which the cells were lysed with 10% 50 μL Triton-X100 solution. A positive control was used to determine the minimum LDH released from apoptosis, in which the cells were cultured on tissue culture polystyrene with no sample.

Statistical analysis

Data sets were evaluated for equal variance using Levene's test and evaluated for normality using the Anderson-Darling test. Once these parameters were established significance was determined using ANOVA with *post hoc* Tukey's test (p value = 0.05). For data sets that did not have equal variance, the Games-Howell test was performed (p value = 0.05). A *post hoc* power analysis was performed on all data sets to verify sample size with a minimum effect size of 0.8. All statistics were performed using Minitab 18.

Results and discussion

Attenuated total reflectance-Fourier transform infrared spectroscopy (ATR-FTIR)

The following peaks seen in all spectra can be attributed to chemical groups found in PP: alkane C–H stretching at 2915 cm^{-1}, methylene group C–H bending at 1455 cm^{-1}, and methyl group C–H bending at 1375 cm^{-1}. Aliphatic ether stretching was expected between 1150–1085 cm^{-1} on the PEG treated samples. However, the small peak seen at 1165 cm^{-1} is unchanged between the control and PEG treated samples. Hydroxyl O–H group stretching is seen at 3550–3200 cm^{-1} and secondary amide N–C═O stretching 1640 cm^{-1} are seen on the HA treated samples. Negative peaks at 2300 cm^{-1} are from background CO_2.

The PEG and sham samples have no differences from the control indicating that the top 1-2 microns of material are predominately PP as seen in Fig. 1. While this indicates that the bulk of the material does not contain PEG, further XPS and contact angle results demonstrate the surface of the material has been altered by the PEG treatment. Due to the known depth of penetration of FTIR (0.5–2 microns)[24] it is possible that a thin layer of PEG is grafted to the surface, yet it does not constitute enough of the material to absorb significant IR waves compared to the PP textile.

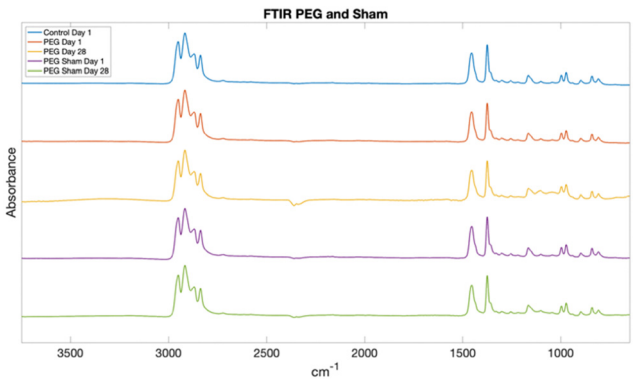

Fig. 1 FTIR curves for PEG and sham samples.

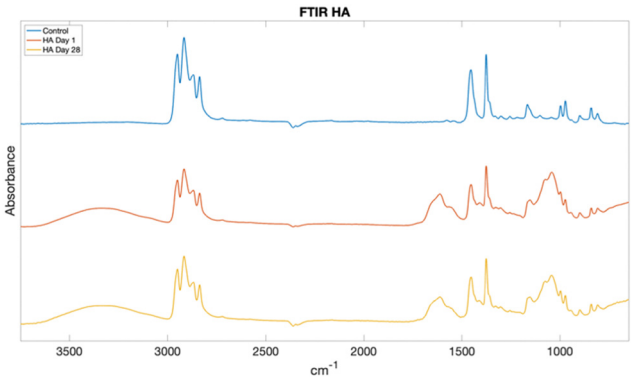

Fig. 2 FTIR curves for HA treated samples.

The HA treated samples have hydroxyl O–H group stretching at 3550–3200 cm^{-1} and secondary amide N–C═O stretching at 1640 cm^{-1} as seen in Fig. 2. This clearly indicates the PP materials have been coated in the crosslinked HA creating a microcomposite on the surface. No change was seen over the 28-day study.

Contact angle goniometry

While contact angle is often used to evaluate 2d surfaces, the method is suitable for determining bulk interactions of a 3d material.[27] Evaluating the PP material for water absorption is crucial if the material can absorb the infectious aerosolized water droplets from respiration.[28,29] Fig. 3–5 shows the control samples and PEG, PEG sham, and HA samples for day 1 and day 28. Controls are shown as reference. Days 7, 14, and 21 can be found in ESI.† PEG and HA treated samples had a significantly lower contact angle than the PP control at all time points. The PEG sham sample did not have a significantly lower contact angle at any time point.

The PEG treated PP samples had consistently lower contact angles than the control PP from day 1 to day 28, however there was a slight increase over that time. The sham samples were

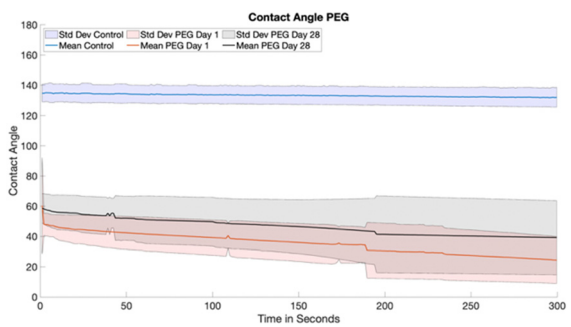

Fig. 3 Contact angle of PEG day 1 (red) day 28 (black) with control reference (blue). Solid lines represent the mean while shading is standard deviation.

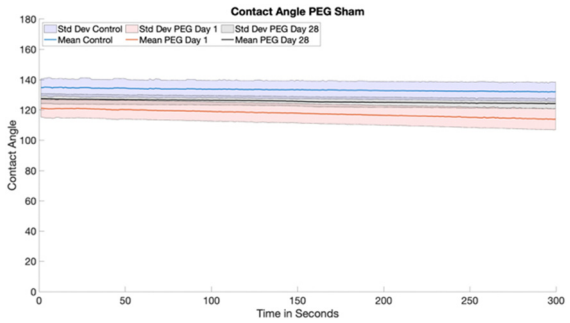

Fig. 4 Contact angle of PEG Sham day 1 (red) day 28 (black) with control reference (blue). Solid lines represent the mean while shading is standard deviation.

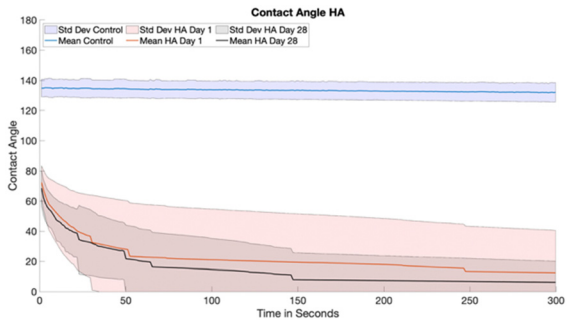

Fig. 5 HA samples at day 1 (red) day 28 (black) with control reference (blue). Solid lines represent the mean while shading is standard deviation.

never significantly different than the controls at any time point. PEG is a hydrophilic polymer and grafting PEG to the PP surface introduced significant hydrophilicity that was retained over the course of 28 days when stored with no protection on a shelf. The sham PEG controls did not have or retain a significantly lower contact angles indicating that the PEG treatment does in fact change the surface chemistry and that the PEG will stay grafted to the sample over 28 days.

The HA treated PP samples had consistently lower contact angles compared to the control from day 1 to 28, with most samples completely absorbing the water droplet over 5 minutes of testing. The results indicate that the HA microcomposite creates a hydrophilic structure on nonwoven PP that is stable for at least 28 days.

X-Ray photoelectron spectroscopy (XPS)

Day 1 results are shown Table 1. The surfaces of the PEG and sham samples have more oxygen compared to the control. Some silicon is seen on the sham, control, and HA samples most likely due to contamination from silicone oils used in the lab vacuum systems and in heating baths. As would be expected, nitrogen and sodium are seen on the HA sample due to the presence of nitrogen in HA and the use of sodium chloride in the hydrolysis process.

Day 28 results are seen in Table 2. The PEG sample and sham sample surfaces continued to maintain significantly

Table 1 Percent elemental composition of day 1 PP samples

Sample	Carbon	Oxygen	Nitrogen	Silicon	Others
PEG	86.3	13.7	0	0	0
Sham	70.42	21.29	1.15	7.14	0
Control	90.15	5.35	0	4.5	0
HA	72.83	19.42	4.89	1.77	1.08(Na)

Table 2 Percent elemental composition of day 28 PP samples

Sample	Carbon	Oxygen	Nitrogen	Silicon	Others
PEG	73.81	24.56	0	0.99	0
Sham	68.69	24.33	0	6.98	0
Control	93.09	4.21	0	2.69	0
HA	60.45	32.23	3.36	0.96	2.83(Na)

higher oxygen to carbon ratios compared to the control over the 28 day study. Interestingly, the PEG sample had almost double the oxygen to carbon ratio at day 28 compared to day 1. HA samples continued to have more oxygen compared to the control and had continued presence of nitrogen and sodium.

The PEG sham maintained a higher oxygen to carbon ratio over the course of the study indicating the oxygen plasma treatment is durable over time but does not induce significant hydrophilicity as seen in the contact angle data. The PEG samples had an increase in the oxygen to carbon ratio on day 28 which may be due to variation in the PEG grafting across the surface. The shifting oxygen ratios did not have a significant effect on the hydrophilicity of the samples as seen in the contact angle data. The oxygen to carbon ratios of the HA samples increased over the study indicating variation across the surface however the presence of nitrogen without great variation indicates the HA treatment is more confluent over the sample. Neither control sample nor the PEG sham sample had a change in the oxygen to carbon ratio indicating there was not contamination that introduced oxygen to the surface. Day 7, 14, and 21 data can be found in ESI.†

Tensile properties

The tensile strain at break (tensile failure) in the nonwoven polypropylene and the Youngs' modulus can be seen in Table 3. The PEG, PEG sham, and control samples did not have statistically different Youngs' moduli. With the exception the of outlying sample, the PEG sham samples did have much greater strain to break (63–75%) compared to the PEG (31–47%) and control (29–39%) samples. The greater strain to break seen in the PEG sham samples may be due to soaking the nonwoven PP in ethanol and methanol allowing the fabric to swell and disentangle. The PEG samples also underwent the soaking process indicating they too should have greater strain to break, however the introduction of the PEG molecules and grafting through plasma treatment most likely resulted in light cross-linking of the disentangled PP. The longevity over 28 days of the PEG as indicated by XPS and contact angle demonstrates the PEG is bound to the PP resulting in the potential for cross-linking the PP fibers.

Table 3 Tensile failure and Youngs' modulus of nonwoven polypropylene samples

Sample	Control	PEG Sham	PEG	HA
Tensile failure (strain %)	29–39	63–75[a]	31–47	18–25
Youngs modulus (MPa)	0.345 ± 0.043	0.271 ± 0.047	0.362 ± 0.058	0.574 ± 0.020

[a] The PEG sham samples had an outlier fail at 27% strain.

The increased modulus and reduced strain to break seen in the HA samples is due to the creation of a secondary network of material being deposited over the surface and that network being crosslinked in place. The crosslinked HA acts to reinforce the material at low strain resulting in a higher modulus but restricts the movement of nonwoven PP fibers resulting in lower strain at break.

Water vapor transmission rate (WVTR)

All treated mask samples had significantly higher WVTR compared to the control during week 1 of testing, with the PEG and HA samples having greater transmission than the PEG sham. The HA and PEG samples had a higher WVTR compared to the control during week 3, with the PEG sham sample having lower transmission. Interestingly, the PEG and PEG sham samples had a higher transmission rate at week 5. While there were differences between samples and weeks, all samples except for the PEG sham had a decreasing WVTR over the study and all maintained high water vapor transmission as would be expected from a porous material. Fig. 6 shows the WVTR results for each sample at day 1, 14, and 28.

The WVTR of the HA samples reduced more compared to PEG and PEG sham treatment and approached the transmission rate of the control samples over the course of the study. It should be noted that except for the PEG sham all samples had a reduction in WVTR, but that the HA samples had the greatest reduction. The most probable reason for this reduction in WVTR is the swelling of the HA microcomposite on the PP fibers caused a reduction of pore sizes of the material. Since the materials were stored in plastic between time points, they were unable to dry. This indicates that the HA treated samples retain water, but not to a degree that prevents breathability. In fact, all samples were either more breathable or not significantly less breathable than the control except the PEG sham after 3 weeks. Considering the importance of breathability in a mask this is a surprising, but positive aspect of these treatments. While the PEG sham was lower after 3 weeks it was not so low as to cause concern. The WVTR results indicate that the PEG and HA treatments do not hinder the breathability of the PP fabric.

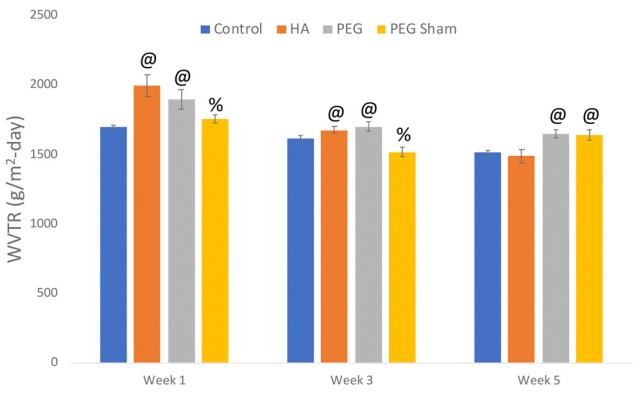

Fig. 6 WVTR results for all timepoints for all treatment groups compared to that week's control sample. Columns sharing a symbol are not statistically different (p value < 0.05, $n = 6$) Column and error bars represent mean ± standard deviation.

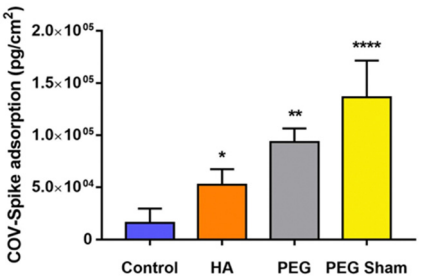

Fig. 7 Spike protein adsorption on nonwoven PP substrates. Asterisks indicates significance ($p = 0.05$). Each sample was significantly different than all other samples as indicated by the different number of asterisks.

Spike protein ELISA

All samples had significantly higher adsorption of the spike protein compared to the control samples. Fig. 7 shows the SARS-COV-2 spike protein adsorption. The significantly greater rates of spike protein adsorption indicate the HA and PEG treatments may be effective ways to treat nonwoven PP to further retain live SARS-COV-2. By preventing the live virus from detaching from a facemask or other PPE material that has SARS-COV-2, surface transmission of the virus may be greatly reduced. Interestingly, the most effective method at adsorbing the spike protein was the PEG sham treatment. This indicates that the addition of active oxygen groups on the surface may be the most ideal way to absorb SARS-COV-2 on the surface of PP, however the other treatment groups were also effective in increasing adsorption. This experiment did not explore irreversible adsorption of the spike protein. Further explorations should include either irreversible adsorption of the protein or more ideally protein activity post adsorption or live virus activity post adsorption. These studies would shed light on these material's ability to trap or inactivate the virus thus increasing the efficacy of wearing a non-woven PP face mask against COVID-19 transmission.

Cytotoxicity assay

All samples had significantly lower cytotoxicity expression than the negative control and were not significantly different than

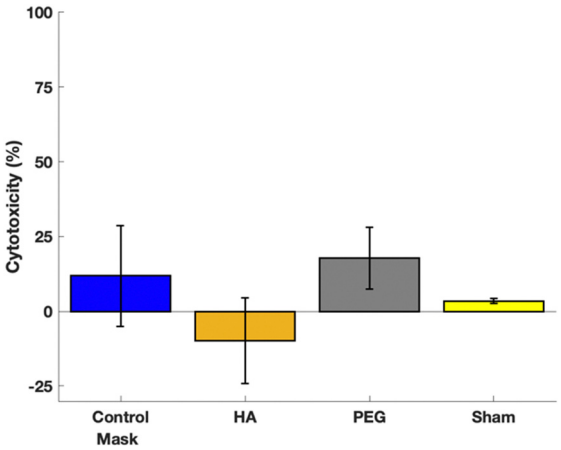

Fig. 8 Cytotoxicity assay results for all treatment groups. All samples were significantly less cytotoxic than the negative control and no different than the positive control (p value < 0.05, n =3). Column and error bars represent mean ± standard deviation.

the positive control. Fig. 8 shows the cytotoxicity test results. This demonstrates that all treatment groups are not cytotoxic, and thus have potential to be used in a skin contacting applications.

Conclusions

All three treatments of the non-woven PP demonstrated increased spike protein adsorption indicating they may help reduce the spread of COVID-19. Interestingly, the PEG sham sample had the greatest protein adsorption indicating the introduction of oxygen through plasma treatment as confirmed by XPS may help reduce COVID-19 transmission.

While the ELISA results are promising, further study using live SARS-CoV-2 virus is warranted, especially because plasma treatment is a simple and low-cost process that may help reduce transmission of SARS-CoV-2.

Conflicts of interest

There are no conflicts to declare.

Acknowledgements

The authors wish to thank the Analytical Resources Core (RRID: SCR_021758) at Colorado State University for instrument access and training. The authors would also like to thank CSU's OVPR office for an exploratory grant. Finally, we would like to thank Cara Leone, Julianne Kindsfater, and Joanna Kindsfater for their help preparing sample treatments.

Notes and references

1 CDC, Coronavirus Disease 2019 (COVID-19). Centers for Disease Control and Prevention **https://www.cdc.gov/coronavirus/2019-ncov/index.html** (2020).
2 CDC, Coronavirus Disease 2019 (COVID-19) PPE. Centers for Disease Control and Prevention **https://www.cdc.gov/coronavirus/2019-ncov/hcp/using-ppe.html** (2020).
3 S. C. Reddy, A. L. Valderrama and D. T. Kuhar, Improving the Use of Personal Protective Equipment: Applying Lessons Learned, *Clin. Infect. Dis.*, 2019, **69**, S165–S170.
4 W. A. Fischer, D. J. Weber and D. A. Wohl, Personal Protective Equipment: Protecting Health Care Providers in an Ebola Outbreak, *Clin. Ther.*, 2015, **37**, 2402–2410.
5 F. S. Kilinc, A Review of Isolation Gowns in Healthcare: Fabric and Gown Properties, *J Eng Fiber Fabr*, 2015, **10**, 180–190.
6 E. Vozzola, M. Overcash and E. Griffing, Environmental considerations in the selection of isolation gowns: A life cycle assessment of reusable and disposable alternatives, *Am. J. Infect. Control*, 2018, **46**, 881–886.
7 N95 Masks Explained|Honeywell, **https://www.honeywell.com/content/honeywell/us/en/newsroom/news/2020/03/n95-masks-explained.html**.
8 T.-N. Lam, *et al.*, Multi-Scale Microstructure Investigation for a PM2.5 Air-Filter Efficiency Study of Non-Woven Polypropylene, *Quantum Beam Sci.*, 2019, **3**, 20.
9 N. van Doremalen, *et al.*, Aerosol and Surface Stability of SARS-CoV-2 as Compared with SARS-CoV-1, *N. Engl. J. Med.*, 2020, **382**, 1564–1567.
10 H. Bui, K. Harris, E. Li, D. Prawel and S. James, The Development and Fabrication of Vapor Crosslinked Hyaluronan-Polyethylene Interpenetrating Polymer Network as a Biomaterial, *ACS Appl. Mater. Interfaces*, 2019, **11**(21), 18930–1894.
11 M. Zhang, R. King, M. Hanes and S. P. James, A novel ultra high molecular weight polyethylene–hyaluronan microcomposite for use in total joint replacements. I. Synthesis and physical/chemical characterization, *J. Biomed. Mater. Res., Part A*, 2006, **78A**, 86–96.
12 P. Li, *et al.*, Exogenous and endogenous hyaluronic acid reduces HIV infection of CD4+ T cells, *Immunol. Cell Biol.*, 2014, **92**, 770–780.
13 H. T. Bui, A. R. Friederich, E. Li, D. A. Prawel and S. P. James, Hyaluronan enhancement of expanded polytetrafluoroethylene cardiovascular grafts, *J. Biomater. Appl.*, 2018, **33**, 52–63.
14 E. Gérard, *et al.*, Surface modifications of polypropylene membranes used for blood filtration, *Polymer*, 2011, **52**, 1223–1233.
15 E. Gérard, E. Bessy, G. Hénard, T. Verpoort and J. Marchand-Brynaert, Surface modification of polypropylene nonwovens with LDV peptidomimetics and their application in the leukodepletion of blood products, *J. Biomed. Mater. Res., Part B*, 2012, **100B**, 1513–1523.
16 D. Ariono and A. K. Wardani, Modification and Applications of Hydrophilic Polypropylene Membrane, *IOP Conf. Ser.: Mater. Sci. Eng.*, 2017, **214**, 012014.
17 L. Zahedi, *et al.*, Development of plasma functionalized polypropylene wound dressing for betaine hydrochloride controlled drug delivery on diabetic wounds, *Sci. Rep.*, 2021, **11**, 9641.

18 M. C. Santos, A. B. Seabra, M. T. Pelegrino and P. S. Haddad, Synthesis, characterization and cytotoxicity of glutathione- and PEG-glutathione-superparamagnetic iron oxide nanoparticles for nitric oxide delivery, *Appl. Surf. Sci.*, 2016, **367**, 26–35.

19 A. Reznickova, *et al.*, PEGylated gold nanoparticles: Stability, cytotoxicity and antibacterial activity, *Colloids Surf., A*, 2019, **560**, 26–34.

20 G. Jiang, J. Sun and F. Ding, PEG-g-chitosan thermosensitive hydrogel for implant drug delivery: cytotoxicity, in vivo degradation and drug release, *J. Biomater. Sci., Polym. Ed.*, 2014, **25**, 241–256.

21 G. Liu, *et al.*, Cytotoxicity study of polyethylene glycol derivatives, *RSC Adv.*, 2017, **7**, 18252–18259.

22 D. A. Prawel, *et al.*, Hemocompatibility and Hemodynamics of Novel Hyaluronan–Polyethylene Materials for Flexible Heart Valve Leaflets, *Cardiovasc. Eng. Technol.*, 2014, **5**, 70–81.

23 S. James, R. Oldinski, M. Zhang and H. Schwartz, UHMWPE–Hyaluronan Microcomposite Biomaterials, *UHMWPE Biomaterials Handbook*, 2016, pp. 412–433, DOI: **10.1016/B978-0-323-35401-1.00023-5**.

24 F. M. Mirabella, *Internal reflection spectroscopy: theory and applications*. (Marcel Dekker, 1993).

25 D13 Committee, Test Method for Tensile Properties of Single Textile Fibers. **http://www.astm.org/cgi-bin/resolver.cgi?D3822D3822M-14R20**, DOI: **10.1520/D3822_D3822M-14R20**.

26 ASTM International – ASTM D6701-16 – Standard Test Method for Determining Water Vapor Transmission Rates Through Nonwoven and Plastic Barriers|Engineering360, **https://standards.globalspec.com/std/3862233/astm-d6701-16**.

27 M. J. Hawker, A. Pegalajar-Jurado and E. R. Fisher, Innovative Applications of Surface Wettability Measurements for Plasma-Modified Three-Dimensional Porous Polymeric Materials: A Review, *Plasma Processes Polym.*, 2015, **12**, 846–863.

28 S. Tang, *et al.*, Aerosol transmission of SARS-CoV-2? Evidence, prevention and control, *Environ. Int.*, 2020, **144**, 106039.

29 M. Klompas, M. A. Baker and C. Rhee, Airborne Transmission of SARS-CoV-2: Theoretical Considerations and Available Evidence, *JAMA*, 2020, **324**, 441–442.